Comparison of Voxel-Based Morphometry (VBM) and Tractography of Diffusion Tensor MRI (DT-MRI) in Temporal Lobe Epilepsy

Maryam Afzali, Hamid Soltanian-Zadeh
Control and Intelligent Processing Center of Excellence,
School of Electrical and Computer Engineering
University of Tehran
Tehran 14395-515, Iran
m.afzali@ece.ut.ac.ir, hszadeh@ut.ac.ir

Hamid Soltanian-Zadeh
Image Analysis Laboratory, Radiology Department
Henry Ford Health System
Detroit, MI 48202, USA
hamids@rad.hfh.edu

***Abstract*— Temporal lobe epilepsy (TLE) is a neurological disease that affects millions of individuals in the world. Majority of TLE patients suffer from refractory seizures. Determining abnormal/damaged regions of the brain that harbor seizure focus is a critical step towards treatment of TLE patients. Diffusion tensor imaging (DTI) is a non-invasive method that we use in this work to determine damaged regions of white matter in the brain. To this end, we apply two methods, voxel based morphometry (VBM) and fiber tracking. We use these methods along with two anisotropy maps (EAR and FA) extracted from the DTI data. We use DTI data of 31 subjects (12 normal subjects and 19 TLE patients) for testing and evaluation studies. The VBM method shows that TLE is associated with reduction of both of FA and EAR values in several regions within the temporal lobes. The tractography method shows abnormal diffusion characteristics in three fiber bundles (fornix, uncinate fasciculus, and cingulum). The results show that the EAR maps are less sensitive to noise than the FA maps and the EAR values change more than the FA values in TLE.**

Keywords- Diffusion Tensor Magnetic Resonance Imaging (DT-MRI); Image Analysis; Medical Imaging; Voxel-Based Morphometry (VBM); Temporal Lobe Epilepsy (TLE); Fractional Anisotropy (FA); Ellipsoidal Area Ratio (EAR)

I. INTRODUCTION

Temporal lobe epilepsy (TLE) is one of the most common types of epilepsy that involves parts of the white matter of the brain [1]. Some of the TLE patients can be treated by resecting their seizure focus. To this end, neurosurgeons need to know the location of the seizure focus. The brain is made of connective networks. If an abnormality occurs in one region, it will affect other regions of the brain. Consequently, TLE causes changes in different parts of the brain network.

Diffusion tensor imaging (DTI) is a new MRI method that can be used to determine the diffusion of water in the brain tissue. In the gray matter and the cerebral spinal fluid (CSF), water diffusion in different directions is almost equal and therefore the diffusion is called isotropic. The white matter of the brain is made of fiber bundles. The fibers have myelin sheaths and cell membranes that restrict diffusion of water across them. Consequently, the diffusion in the direction perpendicular to the main axes of the fiber is small but the diffusion along the main axes is large. Therefore, the diffusion ellipsoid is not spherical. It is stretched along the main axes of the fiber. In this case, the diffusion is anisotropic. The diffusion ellipsoid contains information about the diffusion anisotropy, which can be quantified. Fractional anisotropy (FA) and the ellipsoidal area ratio (EAR) [2] are two indices used in this paper to quantify diffusion.

There are different methods to analyze diffusion abnormality in patients compared to controls. One category of methods is region of interest (ROI) based methods [3]. In these methods, the operator determines one or more ROIs so that further analyses are done on these ROIs. The studies using ROIs have shown changes in the hippocampi of the TLE patients. ROI based methods are very sensitive to the regions determined by the operator. To overcome this limitation, methods like tract based spatial statistics (TBSS) and voxel-based morphometry (VBM) that work on the entire brain can be applied. In our previous work, we applied the TBSS method [4, 5] to find abnormalities in the brains of the TLE patients.

In this paper, we apply the VBM method to evaluate changes in the brains of the TLE patients. In this method, the DTI data must be spatially normalized to an atlas. To this end, we smooth the data to stabilize the registration process [1]. In addition, we track the fibers to extract and analyze the bundles involved in the TLE (fornix, cingulum, uncinate fasciculus). We use the mean values of the FA and the EAR parameters of the fiber bundles as the DTI features to separate patients from controls [6]. Finally, we compare the results of the two methods and conclude the work.

II. METHODS

The VBM and fiber tracking methods are applied in this research. Before their applications, some preprocessing steps are done. The images used in this research are diffusion-weighted and non-diffusion weighted images in the DICOM

format. For calculating the tensor (D), the following equation is used.

$$D = \ln(I_0 / I_q) \times b^{-1} \quad (1)$$

where I_0 is the image intensity without a diffusion gradient and I_q is the image intensity for the diffusion gradient q. The matrix b is calculated by:

$$b = \gamma^2 G^2 \delta^2 (\Delta - \delta/3) \quad (2)$$

where γ is the gyromagnetic ratio, G is the strength of the gradient pulse, δ is the duration of the pulse, and Δ is the time between the two pulses [7]. The tensor D is denoted by the following symmetric 3×3 matrix:

$$D = \begin{bmatrix} D_{xx} & D_{xy} & D_{xz} \\ D_{yx} & D_{yy} & D_{yz} \\ D_{zx} & D_{zy} & D_{zz} \end{bmatrix} \quad (3)$$

After the tensor is estimated, we find its eigenvalues and eigenvectors such that:

$$DV = \lambda V \quad (4)$$

where V is the eigenvector corresponding to the eigenvalue λ which is a scalar constant.

For the 3×3 matrix D, there are 3 orthogonal eigenvectors and their corresponding eigenvalues that can be found by solving the following equations.

$$\det(D - \lambda I) = 0 \quad (5)$$

$$(D - \lambda I)V = 0 \quad (6)$$

After finding the eigenvalues (λ_1, λ_2, λ_3) where λ_1 is the largest eigenvalue, the FA and EAR maps are estimated using the following equations.

$$FA = \sqrt{\frac{(\lambda_1 - \lambda_2)^2 + (\lambda_2 - \lambda_3)^2 + (\lambda_3 - \lambda_1)^2}{2 \times (\lambda_1^2 + \lambda_2^2 + \lambda_3^2)}} \quad (7)$$

$$EAR = 1 - (\frac{1}{3} \times \frac{1}{\lambda_1^{2p}} (\lambda_1^p \lambda_2^p + \lambda_3^p \lambda_2^p + \lambda_1^p \lambda_3^p))^{\frac{1}{p}} \quad (8)$$

where p is a constant. The estimation of EAR has the least error when $p \approx 1.6075$ [2].

A. VBM Analysis

Voxel based morphometry (VBM) is a common approach for studying structural images. It finds the image differences between two groups of subjects. To apply VBM to the DTI data, we do the following steps.

- First, the FA maps are registered to a standard atlas. Then, the aligned FA images are averaged to create a registration template.
- Then, the subjects' FA maps are registered to this template.
- Next, the images are smoothed to overcome adverse effects of minor remaining misalignments. The full width at half maximum of the filter is 8 mm.
- After the smoothing, statistical analysis of the results is carried out. For this purpose, the 2-sample t-test is applied to each voxel to test whether the means are different. This test calculates

$$t = \frac{X_1 - X_2}{S_{x1x2} \sqrt{1/n_1 + 1/n_2}} \quad (9)$$

$$S_{x1x2} = \frac{\sqrt{(n_1 - 1)S_{x1}^2 + (n_2 - 1)S_{x2}^2}}{n_1 + n_2 - 2} \quad (10)$$

where X_1 and X_2 are the mean values of the two groups, n_1 and n_2 are the number of data points in each group, S_x is the variance, and $n - 1$ is the number of degrees of freedom for either group, and the total sample size minus two is the total number of degrees of freedom.

- The result of the statistical analysis is a T map that shows the differences between the control and the patient group.

The above steps are also done for the EAR maps.

B. Fiber Tracking

We track the fibers using the continuous tracking (FACT) algorithm, which is implemented in the DTIstudio software [8, 9]. The steps of this algorithm are as follows.

First, we set thresholds for the FA value and the angle between the eigenvectors of the neighboring voxels. Then, we start the tracking from a voxel that has an FA value larger than the threshold. The direction of the fiber is determined by the principle eigenvector of the diffusion tensor. At the voxel's boundary, the tracking direction is changed to the principle direction of the next voxel. If the FA value is less than the threshold or the angle between the two eigenvector is greater than the threshold, the tracking stops [10]. To find the intersection point of a three dimensional fiber and the boundary of the voxel, we use:

$$x = x_0 + v_x s$$
$$y = y_0 + v_y s \quad (11)$$
$$z = z_0 + v_z s$$

where $\mathbf{v} = (v_x, v_y, v_z)$ is the principal eigenvector, $\mathbf{x_0} = (x_0, y_0, z_0)$ is the starting point and $\mathbf{x} = (x, y, z)$ is the intersection point where the fiber leaves the current voxel and enters the next voxel.

There is a problem in assigning the direction of the new eigenvector, because it may be positive or negative. We find the inner product between it and the present vector. If the result is positive, we keep the sign of the new eigenvector. Otherwise, we reverse it.

Tracking is carried out in the forward and backward directions in order to have complete fiber trajectory. In addition, the lengths of the fibers are compared to a predefined threshold to remove those with lengths smaller than the threshold.

The steps of algorithm can be summarized as follows.

a. Set thresholds for the FA values.

b. Start from a seed point $\mathbf{x}_0$ with an FA value greater than the threshold.

c. Choose the eigenvector $\mathbf{v}$ at $\mathbf{x}_0$ as the current direction.

d. Find the intersection point $\mathbf{x}$ of the fiber and the boundary of the voxel by (11).

e. If the fiber hits the boundary of the image block, go to step (j).

f. If the FA of the new voxel associated with $\mathbf{x}$ is less than the threshold, go to step (j).

g. Calculate the inner product between the current and new eigenvectors and swap the sign of the new eigenvector if the result is negative.

h. If the angle between the current direction $\mathbf{v}$ and new direction associated with $\mathbf{x}$ is greater than the threshold, go to (j).

i. Assign $\mathbf{x}$ to $\mathbf{x}_0$, and go to step (c).

j. Restart from the original seed point $\mathbf{x}_0$, swap the eigenvector $\mathbf{v}$ at $\mathbf{x}_0$, and perform tracking in the reverse direction from step (c) again. If tracking is completed for both directions, proceed to the next step.

k. Combine the tracking results of both directions from the seed point to produce a coordinate chain for the fiber. If it passes the minimum fiber length test, then perform 3D-curve interpolation and smoothing and then create an attribute table with the fiber chain.

l. Apply a-k iteratively until all of the voxels are processed.

m. Create an index matrix with the same size of the original image, in which each voxel stores the pointers to the fiber chains that penetrate this voxel.

After fiber tracking, we determine appropriate ROIs to extract three fiber bundles (cingulum, fornix, uncinate fasciculus) that may be affected by temporal lobe epilepsy. Finally, we calculate the mean values of FA and EAR maps in each of these fiber bundles and use them in the statistical t-tests.

III. Experimental Results

A. Subjects

We studied DT-MRI data of 19 patients with TLE (11 with abnormality in the left temporal lobe and 8 with abnormality in the right temporal lobe) and 12 normal control subjects. DT-MRI data were acquired with 26 gradient directions on a 3T MRI system (GE Medical Systems, Milwaukee, WI, USA) at Henry Ford Hospital, Detroit, MI, USA. For each subject, forty axial slices with 2.6 mm thickness and 256×256 matrix size were acquired.

B. Data Analysis

VBM Results: Figs. 1-2 show the results of the VBM method using the FA and EAR maps, respectively. Note that the damaged areas of the brain are dominantly in the temporal lobes, corpus callosum, and fornix. Details of the results are listed in TABLEs I-II, where the number of voxels in each cluster and the T values are presented. The results indicate that while both of the FA and EAR maps show similar areas, the EAR seems to be more sensitive to tissue damage than the FA.

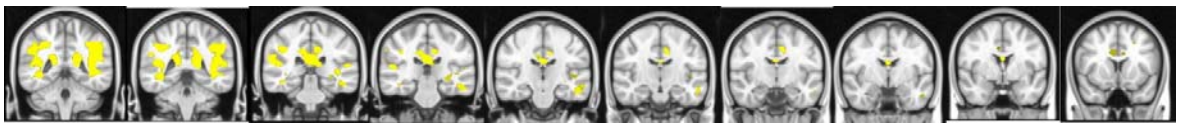

Figure 1. The VBM results obtained using the FA maps. Yellow regions show the damaged areas in TLE. Background is MNI152.

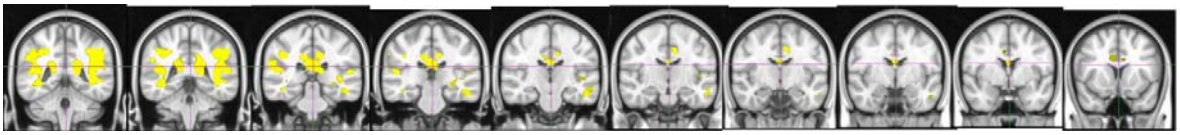

Figure 2. The VBM results obtained using the EAR maps. Yellow regions show the damaged areas in TLE. Background is MNI152.

TABLE I. THE VBM ANALYSIS RESULTS FOR THE LEFT HEMISPHERE.

EAR Reduction	FA Reduction
inferior temporal gyrus (T = 6.41, 9 Voxels)	inferior temporal gyrus (T = 6.87, 7 Voxels)
middle temporal gyrus (T = 6.78, 11 Voxels)	middle temporal gyrus (T = 6.12, 13 Voxels)
superior temporal gyrus (T = 7.71, 9 Voxels)	superior temporal gyrus (T = 6.39, 8 Voxels)
corpus callosum (T = 4.34, 31 Voxels)	crus of fornix (T = 5.43, 23 Voxels)
external capsule (T = 5.17, 36 Voxels)	inferior frontal gyrus (T = 5.77, 15 Voxels)
parahippocampal gyrus (T = 6.37, 40 Voxels)	superior frontal gyrus (T = 6.61, 13 Voxels)
crus of fornix (T = 6.58, 19 Voxels)	corpus callosum (T = 6.69, 34 Voxels)
inferior frontal gyrus (T = 6.47, 9 Voxels)	external capsule (T = 4.79, 29 Voxels)
superior frontal gyrus (T = 8.11, 14 Voxels)	parahippocampal gyrus (T = 7.63, 37 Voxels)
post-central gyrus (T = 6.36, 17 Voxels)	

TABLE II. THE VBM ANALYSIS RESULTS FOR THE RIGHT HEMISPHERE.

EAR Reduction	FA Reduction
inferior temporal gyrus (T = 6.41, 9 Voxels)	middle temporal gyrus (T = 7.41, 11Voxels)
middle temporal gyrus (T = 7.22, 9 Voxels)	superior temporal gyrus (T = 6.13, 12Voxels)
superior temporal gyrus (T = 6.93, 10 Voxels)	corpus callosum (T = 5.77, 37Voxels)
anterior corpus callosum (T = 6.59, 32 Voxels)	external capsule (T = 6.31, 25Voxels)
external capsule (T = 5.11, 25 Voxels)	crus of fornix (T = 6.16, 16Voxels)
crus of fornix (T = 6.67, 18 Voxels)	inferior frontal gyrus (T = 6.75, 9Voxels)
inferior frontal gyrus (T = 5.45, 7 Voxels)	parahippocampal gyrus (T = 5.97, 41Voxels)

Fiber Tracking Results: Three fiber bundles (cingulum, fornix, uncinate fasciculus) are extracted and investigated in this study. To extract these bundles, we use the DTIstudio software in which the fiber bundles are constructed based on the regions of interest (ROIs) that the fiber bundles pass through. For the cingulum, we define two ROIs. The first one is placed on the coronal slices where the cingulum fibers are perpendicular. The second one is placed on the axial slices where the cingulum fibers track from the parietal to the medial temporal region. The second ROI is used to refine the fibers that pass through the first ROI. To this end, the AND operation is applied to the fibers that pass through the two ROIs. The ROIs and the resulting fiber bundles are shown in Figs. 3-4.

The fornix bundle is extracted using an ROI placed on a coronal image as shown in Fig. 5. A 3D view of the fornix fiber bundle is shown in Fig. 6. The uncinate fasciculus is a fiber bundle that connects the frontal and temporal lobes. An ROI used to reconstruct this fiber bundle is shown in Fig. 7. A 3D view of this fiber bundle is presented in Fig. 8.

After fiber tracking, we calculate the mean FA and EAR of each fiber. Then, we apply the t-test on the mean values to determine the fiber bundles and the parameters that discriminate the groups. Finally, the results are used for data clustering.

The results of the t-test are presented in TABLEs III-V. TABLE III shows the results of comparing the control and the left TLE patients. Note that the FA values of the right and left cingulum (R_CG, L_CG) and the right uncinate fasciculus (R_UF) discriminate the two groups (their p-values are less than 0.05). Similarly, the EAR values of the R_CG, R_F, and R_UF discriminate the two groups. For the comparison between the right TLE patients and the controls (TABLE IV), the FA values of the R_CG, L_CG, R_F, and R_UF and the EAR values of the R_UF discriminate the two groups.

Another comparison is done between the right and left TLE patients. In this comparison, the EAR of the R_F is the only parameter that discriminates the two groups. Details are presented in TABLE V. The clustering results of some of the features identified by the t-test analysis are shown in Figs. 9-11. They confirm the discrimination capability of the proposed indices extracted from the DT-MRI data by the fiber tracking method.

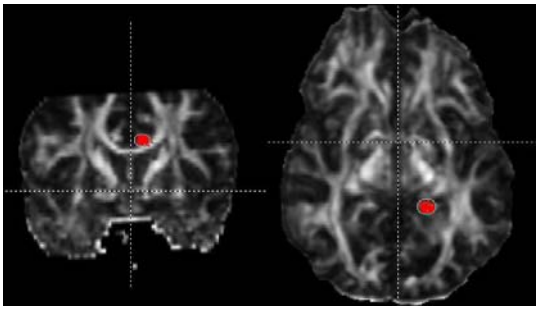

Figure 3. The first ROI for the cingulum is drawn in red on the coronal plane (left image). The second ROI is drawn in red on the axial plane (right image).

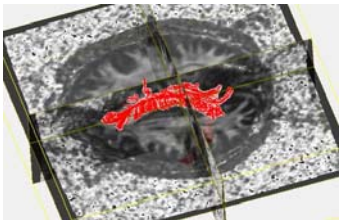

Figure 4. The cingulum fiber bundle extracted using the DTIstudio software.

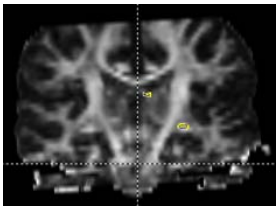

Figure 5. An ROI is selected on a coronal image to extract the left fornix fiber bundle.

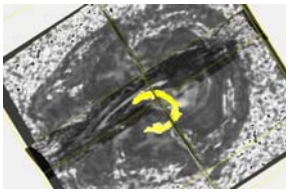

Figure 6. The fornix fiber bundle in 3D.

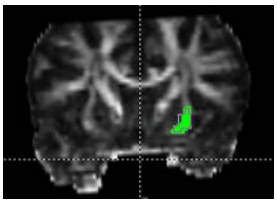

Figure 7. An ROI used to extract the uncinate fasciculus bundle.

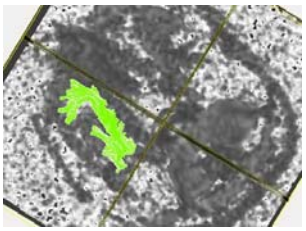

Figure 8. The uncinate fasciculus fiber bundle in 3D.

TABLE III. COMPARISON OF THE CONTROL AND THE LEFT TLE USING THE THREE FIBER BUNDLES

	R_CG [a] (FA)	L_CG [b] (FA)	R_F [c] (FA)	L_F (FA)	R_UF [d] (FA)	L_UF (FA)	R_CG (EAR)	L_CG (EAR)	R_F (EAR)	L_F (EAR)	R_UF (EAR)	L_UF (EAR)
t	6.03	4.14	0.48	-0.55	-3.74	-1.91	3.48	1.22	2.28	-0.06	-2.58	0.039
p	5.48e-06	4.63e-04	0.63	0.58	0.0012	0.07	0.0022	0.233	0.0328	0.952	0.0175	0.968

a. Right Cingulum
b. Left Cingulum
c. Fornix
d. Uncinate Fasciculus

TABLE IV. COMPARISON OF THE CONTROL AND THE RIGHT TLE USING THE THREE FIBER BUNDLES

	R_CG (FA)	L_CG (FA)	R_F (FA)	L_F (FA)	R_UF (FA)	L_UF (FA)	R_CG (EAR)	L_CG (EAR)	R_F (EAR)	L_F (EAR)	R_UF (EAR)	L_UF (EAR)
t	1.9031	2.1416	-2.4157	-2.049	-5.15	-1.93	-0.034	-0.6424	-1.2268	-1.2801	-2.9982	-1.4643
p	0.0731	0.0462	0.026	0.0553	6.69e-05	0.068	0.972	0.5287	0.2357	0.2168	0.0077	0.1604

TABLE V. COMPARISON OF THE LEFT AND RIGHT TLE USING THE THREE FIBER BUNDLES

	R_CG (FA)	R_F (FA)	R_UF (FA)	R_CG (EAR)	R_F (EAR)	R_UF (EAR)	L_CG (FA)	L_F (FA)	L_UF (FA)	L_CG (EAR)	L_F (EAR)	L_UF (EAR)
t	0.7327	2.0941	1.3590	1.8582	2.4838	1.1544	0.4346	1.2219	0.5098	1.1271	1.0533	0.6968
p	0.4737	0.0515	0.1919	0.0805	0.0237	0.2643	0.6693	0.2384	0.6168	0.2753	0.3069	0.4939

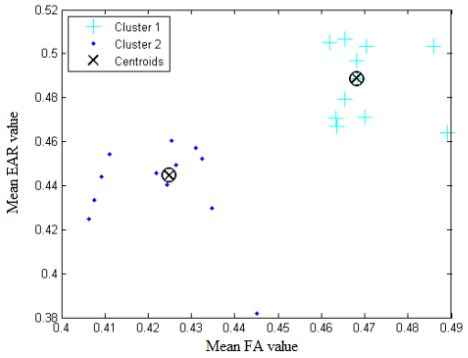

Figure 9. The clustering results of the R_CG and L_CG values of the control and left TLE patients.

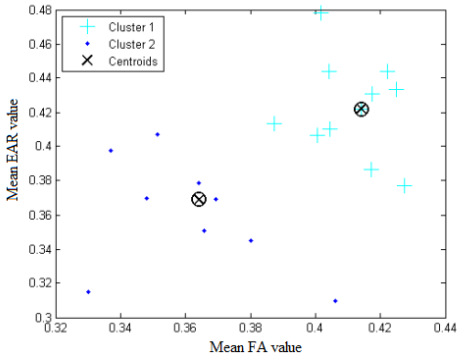

Figure 10. The clustering results of the R_F and R_UF values of the control and right TLE patients.

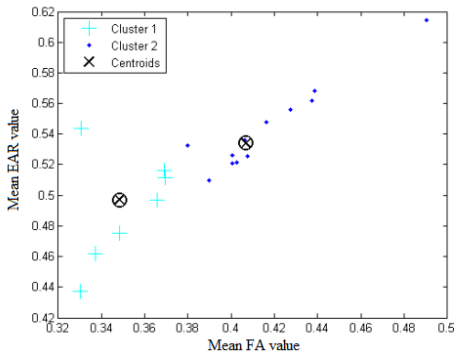

Figure 11. The clustering results of the R_F values of the right and left TLE patients.

IV. Discussion

In this work, we applied advanced image and statistical analysis tools to the DT-MRI data to investigate the changes that may occur in the brains of the TLE patients. We benefited from two image analysis methods and compared the results for two anisotropy indices (FA and EAR). From a theoretical point of view, an advantage of the VBM method is that it does not need ROIs and thus is free of the bias related to the ROI selection process. Nevertheless, it has some limitations. In VBM, each voxel should match among all subjects, which is practically very difficult to achieve. Consequently, smoothing is applied which causes undesirable partial volume effects. Furthermore, all voxels should be processed, requiring a large number of computations for statistical analysis.

On the other hand, the tractography method used in this work is an ROI-based method, focusing on three fiber bundles. As such, its statistical analysis is simpler than that of the VBM.

The VBM results obtained in this work are consistent with the TBSS results obtained in our previous work. The difference between the two results is that the regions generated by the VBM method are extensive while those generated by the TBSS method were thin because the white matter was projected onto its skeleton.

The final results depend on the anisotropy indices in addition to the analysis methods discussed above. In this work, we use two indices, FA and EAR. FA is a common anisotropy index used extensively in the literature. EAR is a new anisotropy index shown to be more robust to noise. Therefore, it is expected to be superior to FA for investigating the damaged regions of the white matter.

The VBM results suggest that the volume of hippocampus changes due to TLE. This is consistent with the changes we found in the parahippocampal gyrus by the TBSS method in our previous work. They are also consistent with the findings of other groups who used ROI-based methods [3]. The inferior frontal gyrus, temporal lobes, and corpus callosum are regions with reduced FA and EAR. These regions were also identified as abnormal regions by the mean diffusivity (MD) and FA in previous work [1]. Moreover, the fiber tracking results using the FA and EAR maps are consistent with those reported in the literature [6].

V. Conclusion

In this paper, we used two anisotropy indices (FA and EAR) for investigating the localized changes that may occur in TLE. For this purpose, we used two methods (VBM and fiber tracking). The results show that there are abnormal regions in a large brain network in the TLE patients. Prominent EAR and FA changes are observed in the temporal lobes and the inferior frontal gyrus. In general, EAR has a number of advantages compared to other diffusion anisotropy indices like FA. It is an approximation of the curvature and surface area of the tensor's ellipsoid that encodes biological characteristics of water diffusion. Therefore, it seems appropriate for studying organization of tissues and fiber tracks in the brain.

References

[1] N. K. Focke, M. Yogarajah, S. B. Bonelli, P. A. Bartlett, M. R. Symms, J. S. Duncan, “Voxel-based diffusion tensor imaging in patients with mesial temporal lobe epilepsy and hippocampal sclerosis,” NeuroImage, vol. 40, pp. 728-737, 2008.

[2] D. Xu, J. Cui, R. Bansal, X. Hao, J. Liu, W. Chen, B. S. Peterson, “The ellipsoidal area ratio: an alternative anisotropy index for diffusion tensor imaging,” Magnetic Resonance Imaging, vol. 27, pp. 311-323, 2009.

[3] N. F. Moran, L. Lemieux, N. D. Kitchen, D. R. Fish, S. D. Shorvon, “Extrahippocampal temporal lobe atrophy in temporal lobe epilepsy and mesial temporal sclerosis,” Brain vol. 124, pp. 167–175, 2001.

[4] S. M. Smith, M. Jenkinson, H. Johansen-Berg, D. Rueckert, T. E. Nichols, C. E. Mackay, K. E. Watkins, O. Ciccarelli, M. Z. Cader, P. M. Matthews, T. E. Behrens, “Tract-based spatial statistics: voxelwise analysis of multi-subject diffusion data,” NeuroImage, vol. 31, pp. 1487–1505, 2006.

[5] M. Afzali, H. Soltanian-Zadeh, “tract based spatial statistical analysis of diffusion parameters in temporal lobe epilepsy”, 16th Iranian conference on biomedical engineering, 30 December 2009.

[6] M. E. Ahmadi, D. J. Hagler, C. R. McDonald, E. S. Tecoma, V. J. Iragui, A. M. Dale, E. Halgren, “Side matters: diffusion tensor imaging tractography in left and right temporal lobe epilepsy,” American Journal of Neuroradiology, vol. 30, pp. 1740-1747, 2009.

[7] E. O. Stejskal “Use of spin echoes in a pulsed magnetic-field gradient to study anisotropic, restricted diffusion and flow,” Journal of Chemical Physics, vol. 43, pp. 3597–3603, 1965.

[8] S. Mori, B. J. Crain, V. P. Chacko, P. C. M. van Zijl, “Three-dimensional tracking of axonal projections in the brain by magnetic resonance imaging,” annals of neurology, vol. 45, pp. 265-269, 1999.

[9] R. Xue, P. C. M. van Zijl, B. J. Crain, M. Solaiyappan, S. Mori, “In vivo three-dimensional reconstruction of rat brain axonal projections by diffusion tensor imaging,” Magn. Reson. Med., vol. 42, pp. 1123-1127, 1999.

[10] H. Jiang, P. C. M. van Zijl, J. Kim, G. D. Pearlson, S. Mori, “DtiStudio: resource program for diffusion tensor computation and fiber bundle tracking,” computer methods and programs in biomedicine, vol. 81, pp. 106–116, 2006.